U.S.N.A.---Trident Scholar project report; no. 326 (2004)

OPTICAL LIMITING IN A SINGLE MODE WAVEGUIDE SYSTEM

by

Midshipman Jeffrey C. Payne, Class of 2004
United States Naval Academy
Annapolis, Maryland

Certificate of Advisor(s) Approval

Assistant Professor James J. Butler
Physics Department

Acceptance for the Trident Scholar Committee

Professor Joyce E. Shade
Deputy Director of Research and Scholarship

REPORT DOCUMENTATION PAGE

Form Approved
OMB No. 074-0188

Public reporting burden for this collection of information is estimated to average 1 hour per response, including g the time for reviewing instructions, searching existing data sources, gathering and maintaining the data needed, and completing and reviewing the collection of information. Send comments regarding this burden estimate or any other aspect of the collection of information, including suggestions for reducing this burden to Washington Headquarters Services, Directorate for Information Operations and Reports, 1215 Jefferson Davis Highway, Suite 1204, Arlington, VA 22202-4302, and to the Office of Management and Budget, Paperwork Reduction Project (0704-0188), Washington, DC 20503.

1. AGENCY USE ONLY (Leave blank)	2. REPORT DATE	3. REPORT TYPE AND DATE COVERED
	7 May 2004	

4. TITLE AND SUBTITLE
Optical limiting in a single mode waveguide system

5. FUNDING NUMBERS

6. AUTHOR(S)
Payne, Jeffrey C. (Jeffrey Christopher), 1981-

7. PERFORMING ORGANIZATION NAME(S) AND ADDRESS(ES)		8. PERFORMING ORGANIZATION REPORT NUMBER

9. SPONSORING/MONITORING AGENCY NAME(S) AND ADDRESS(ES)		10. SPONSORING/MONITORING AGENCY REPORT NUMBER
US Naval Academy Annapolis, MD 21402		Trident Scholar project report no. 326 (2004)

11. SUPPLEMENTARY NOTES

12a. DISTRIBUTION/AVAILABILITY STATEMENT	12b. DISTRIBUTION CODE
This document has been approved for public release; its distribution is UNLIMITED.	

13. ABSTRACT: The objective of this Trident project is to study the optical properties of single mode waveguide systems that exhibit an absorption that increases with the intensity of the light incident upon them. In this way these devices limit the transmission of optical energy and are referred to as “optical limiters”. Such systems are of great value to both the military and the telecommunications industry because of their ability to protect sensitive equipment from exposure to high intensity light. Experiments were performed using very small glass capillaries filled with materials that exhibit a nonlinear absorption. In this case, the materials absorb a greater amount of light as the intensity increases. These systems act as waveguides, confining the light to a small “core” region where the nonlinear material resides. Furthermore, only one intensity distribution (or “mode”) is allowed if the index of refraction of the core is very close to that of the surrounding glass. In this case, the waveguide is called “single mode”. Single mode behavior was achieved by controlling the temperature of the waveguide in order to tune the index of refraction of the core material. Pulses of visible light (wavelength = 532 nm, pulse width = 4ns) were coupled into single mode waveguides and the input and output intensities were measured. These results were compared to optical limiting observed in multi-mode waveguides. It was observed that multi-mode waveguides exhibit better optical limiting than single-mode waveguides. This is because the entire mode structure is confined to the core in a multi-mode waveguide. However, a portion of the mode extends into the cladding in a single-mode waveguide. In addition, single-mode waveguides show a decreased ability to limit at higher temperatures where the difference in index of refraction is smallest. At these temperatures the relative amount of light in the nonlinear core is decreasing, leading to a reduction in optical limiting.
.
.

14. SUBJECT TERMS: optical limiting, single-mode waveguide, reverse-saturable absorption, optical nonlinearity	15. NUMBER OF PAGES 56
	16. PRICE CODE

17. SECURITY CLASSIFICATION OF REPORT	18. SECURITY CLASSIFICATION OF THIS PAGE	19. SECURITY CLASSIFICATION OF ABSTRACT	20. LIMITATION OF ABSTRACT

Abstract

The objective of this Trident project is to study the optical properties of single mode waveguide systems that exhibit an absorption that increases with the intensity of the light incident upon them. In this way these devices limit the transmission of optical energy and are referred to as "optical limiters". Such systems are of great value to both the military and the telecommunications industry because of their ability to protect sensitive equipment from exposure to high intensity light.

Experiments were performed using very small glass capillaries filled with materials that exhibit a nonlinear absorption. In this case, the materials absorb a greater amount of light as the intensity increases. These systems act as waveguides, confining the light to a small "core" region where the nonlinear material resides. Furthermore, only one intensity distribution (or "mode") is allowed if the index of refraction of the core is very close to that of the surrounding glass. In this case, the waveguide is called "single mode". Single mode behavior was achieved by controlling the temperature of the waveguide in order to tune the index of refraction of the core material. Pulses of visible light (wavelength = 532 nm, pulse width = 4ns) were coupled into single mode waveguides and the input and output intensities were measured. These results were compared to optical limiting observed in multi-mode waveguides.

It was observed that multi-mode waveguides exhibit better optical limiting than single-mode waveguides. This is because the entire mode structure is confined to the core in a multi-mode waveguide. However, a portion of the mode extends into the cladding in a single-mode waveguide. In addition, single-mode waveguides show a decreased ability to limit at higher temperatures where the difference in index of refraction is smallest. At these temperatures the relative amount of light in the nonlinear core is decreasing, leading to a reduction in optical limiting.

Keywords: optical limiting, single-mode waveguide, reverse-saturable absorption, optical nonlinearity

Acknowledgements

I would like to take this opportunity to thank those who have supported me during this Trident Project research. In particular, I would like to thank my project advisor, Dr. James Butler for his commitment to this particular project and for his devotion to enhancing research opportunities at the Naval Academy. Without his guidance, expertise, and patience, progress in this endeavor would not have been possible.

In addition, I would like to thank my family for their love and support throughout my career at the Naval Academy. I have no doubt that my drive to succeed was imbued in me by my father's persistent demands of excellence, while my sanity maintained by my mother's care and understanding.

Furthermore, I would like to thank those who have thus far collaborated with me on this project. The expertise of Dr. Jim Shirk, Dr. Richard Pong, and Dr. Steven Flom have provided this project a unique perspective from which to better access and overcome difficulties.

I would also like to thank Mr. Michael Gerhart, Dr. Frank Herron, and all others associated with the Reading-Berks Science and Engineering Fair. Without this forum in which to explore my scientific interests at an early age, it is unlikely that I would have been motivated to pursue research at the Naval Academy.

Finally, I would like to thank Dr. William Heffner. As a high school sophomore I searched for a mentor to guide and assist me with a science fair project and could not have found a better one. His willingness to sacrifice his time and energy to the pursuit of scientific discovery with a teenager he had just met not only inspired me to pursue further optical research, but also deepened my respect for those who sacrifice their time for the betterment of others.

Table of Contents

1. Introduction

In recent years, technological advances, coupled by aggressive expansion of the telecommunication industry, have lead to an increased interest in the properties of optical waveguide systems. One particularly interesting property that can, under certain conditions, occur in such systems is a phenomenon known as *optical limiting*. These systems are used to keep the optical intensity below the threshold for damage of sensitive optical devices. At low intensity inputs, the intensity of the output light will increase linearly. However, when the input intensity reaches a certain level, the output intensity will increase more slowly than the intensity of the input light. Clearly, this is advantageous for any fiber optic system that delivers an optical signal to equipment that could be damaged by high intensity light. In addition, it has been suggested that such a system could be used to protect the eyes of soldiers on the battlefield from the effects of laser weapons.[1]

Optically nonlinear materials are nearly ideal for optical limiting applications due to their fast response time (on the order of nanoseconds or picoseconds). In such materials, either the index of refraction (and thus the speed of light in the medium) or the optical absorption is a function of intensity.

In order for nonlinear optical limiters to be practical in fiber optic systems, they must be able to be easily integrated into those systems. For instance, filling the core of an optical waveguide with such a substance allows one to limit the intensity transmitted by that waveguide. Many waveguides are large enough to allow light to transmit in a multitude of optical modes. Each mode corresponds to an allowed distribution of light within the waveguide core. However, there are waveguides with appropriately designed physical characteristics such that only a single mode (the so-called “fundamental mode”) is transmitted. Single-mode waveguides are

commonly used in telecommunications industry. Therefore, optical limiters that are compatible with single-mode waveguides have the potential for a tremendous number of applications. To the best of the author's knowledge, no one has yet demonstrated optical limiting in a single-mode fiber.

This study examines optical limiting in a single-mode waveguide system in an effort to understand single-mode optical limiting at various temperatures and to compare single-mode limiting to the optical limiting observed in multi-mode systems.

2. Background

A. Optical limiting

Optical limiting systems limit the maximum intensity (power density) of light that is transmitted from that system. At low input intensities, there is a linear relationship between the system's input and output light intensities. However, at higher input intensities, the intensity of the output light increases more slowly than the intensity of the input light. This behavior is an example of optical *nonlinearity*. In addition to describing optical nonlinearity in terms of light intensity, this phenomenon can also be discussed in terms of energy density or *fluence*. The two optical properties that commonly exhibit nonlinear behavior are absorption and index of refraction. The input fluence at which significant optically nonlinear effects emerge is known as the system's *limiting threshold*. The limiting threshold is commonly defined as the input fluence at which the transmitted fluence decreases by a factor of two from the value predicted in the linear regime.[2]

1. Nonlinear absorption

In this project, materials will be used that exhibit the property of nonlinear absorption. When light is incident on a material, the material will absorb some of that light. A material's ability to absorb light is characterized by its absorption coefficient (α). The absorption coefficient can be described mathematically as[3]:

$$\alpha = \alpha_0 + \alpha_1\left(\frac{E_0^2}{2\mu_0 c}\right) \quad (1)$$

where $\frac{E_0^2}{2\mu_0 c}$ is the intensity of the incident light, E_0 is the electric field amplitude, μ_0 is the permeability of free space, c is the speed of light in a vacuum, α_0 is the linear coefficient of absorption, and α_1 is the nonlinear coefficient of absorption. At low input intensities the absorption coefficient will be dominated by the linear term. However, as the intensity increases the nonlinear term will become significant. There are a number of processes by which nonlinear absorption can occur. Two such processes, two-photon absorption (TPA) and reverse-saturable absorption (RSA), are common in optical limiting materials and will be discussed in detail.

a. Two-Photon Absorption (TPA)

Figure 1 illustrates TPA. Light of frequency ν is incident on an atom. Each photon of light carries an energy E=hν where h is Planck's constant. In TPA, the atom cannot be elevated to an excited energy state (L_1) by the energy imparted to it by a single photon. However, it is elevated from its ground state (L_0) when two photons strike the atom simultaneously.[4] The absorption cross-section (σ) characterizes the likelihood that this effect will occur. Unlike in

linear optics where σ is a constant, nonlinear optics tells us that the absorption cross-section increases with light intensity according to the equation:

$$\sigma=\sigma^{(2)}I \qquad (2)$$

where $\sigma^{(2)}$ is a coefficient describing two-photon absorption and I is the intensity of the incident light.[4] This makes sense when one considers that higher intensity light contains a greater number of photons in a given time, making the probability of two photons simultaneously striking a particular atom greater.

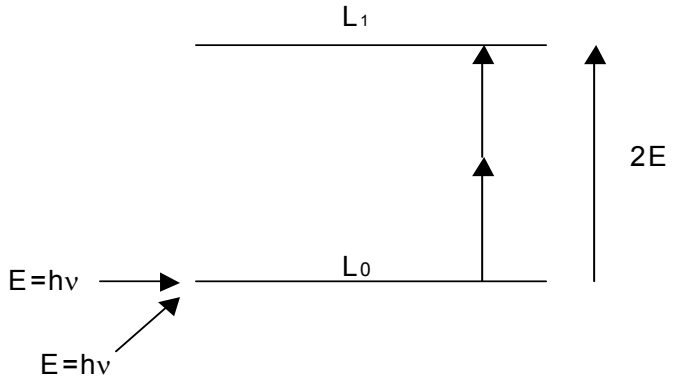

Figure 1 depicts two photons of energy hν simultaneously striking an electron in its ground state and exciting it to its first excited state. This process is known as Two-Photon Absorption (TPA).

b. Reverse-Saturable Absorption (RSA)

Figure 2 illustrates RSA. Unlike the case of TPA, in which one atom absorbs two photons simultaneously, RSA is caused by one atom making two distinct photon absorptions. When an atom in its ground state (L_0) absorbs a photon with sufficient energy, it is elevated to its first excited energy state (L_1). The ground state cross section (σ_g) characterizes the likelihood that such a transition will occur. Likewise, when the first excited energy state becomes populated with a sufficient number of electrons, those electrons can absorb another photon and

be elevated to the second energy level (L_2). The likelihood of this occurring is characterized by the excited state cross section (σ_e). In a material that exhibits RSA, σ_e will be much greater than σ_g. It is in this second excited state that the electron will lose energy through other processes (such as collisions with neighboring molecules). As a result, the absorption coefficient increases with the intensity of the incident light. As the nomenclature suggests, this is the opposite effect of that exhibited by saturable absorbers, in which σ_g is greater than σ_e, leading to a decrease in absorption coefficient.

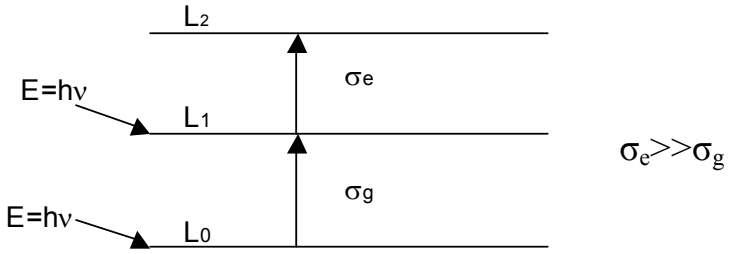

Figure 2 depicts the two distinct electron excitations that result in Reverse-Saturable Absorption (RSA). The ground state cross-section (σ_g) and the excited state cross-section (σ_e) indicate the likelihood that a transition will occur.

Furthermore, it is important to understand the relationship between a molecular absorption cross section and its related coefficient of absorption. When light is incident upon an RSA material, a portion of the molecules are excited to the first excited state (L_1) while other molecules remain in their ground state (L_0). The molecules in the excited state exhibit a different absorption coefficient than those in the ground state. Thus, the two groups much be treated individually when expressing the overall coefficient of absorption of the material.[5]

The coefficient of absorption related to the ground-state molecules is given by[7]:

$$\alpha_g = \sigma_g C_1 N_A \frac{1L}{1000mL} \qquad (3)$$

where C_1 is the molar concentration (mol/L) of the molecules remaining in their ground state and N_A is Avogadro's number.

The coefficient of absorption related to molecules in their excited state is similarly described[6]:

$$\alpha_e = \sigma_e C_2 N_A \frac{1L}{1000mL} \qquad (4)$$

where C_2 is the molar concentration (mol/L) of excited molecules.

The overall coefficient of absorption is the sum of these two expressions[5]:

$$\alpha = \alpha_g + \alpha_e \qquad (5)$$

As light energy strikes the solution, more and more molecules will reach their excited state. Eventually, the excited molecules will so exceed the ground-state molecules that the excited-state coefficient of absorption will dominate the absorption expression. In the excited-state, energy is dissipated by collisions with other molecules and various other processes.[5]

2. Nonlinear Refraction

The manner in which light propagates through a material is characterized by the material's *index of refraction*. Index of refraction is defined as:

$$n = \frac{c}{v} \quad (6)$$

where n is the index of refraction, c is the speed of light in a vacuum, and v is the speed at which light propagates in a medium.

The materials that will be utilized in this study exhibit nonlinear refraction. Nonlinear refraction can be described in a fashion similar to the nonlinear description of coefficient of absorption (shown in equation 1). That is:

$$n = n_0 + n_1\left(\frac{E_0^2}{2\mu_0 c}\right) \quad (7)$$

where n_0 is the linear index of refraction and n_1 is the nonlinear index of refraction. When an absorptive medium is irradiated by a light source, the absorbed optical energy can be converted through collisions and other nonradiative processes. This increase in thermal energy leads to an increase in temperature. As the material heats up it becomes less dense, decreasing the refractive index and increasing the speed of light through the material. Therefore, it follows that materials that undergo nonlinear absorption also exhibit thermal nonlinear refraction.[5]

B. Nonlinear Materials

As the nomenclature suggests, nonlinear optical materials are materials that exhibit nonlinear absorption or refraction. The optical limiting effects that result from such behavior make these materials ideal candidates for a variety of applications, including protective buffers between an input optical signal and highly sensitive equipment. Furthermore, such materials are compatible with fiber optic systems, making them particularly important to the telecommunications industry. This study will examine optical limiting in a waveguide system that consists of an outer glass cladding and an inner core filled with an optically nonlinear material. The nonlinear optical material silicon naphthalocyanine (SiNc) that will be used in this project is a reverse-saturable absorber (RSA). However, equation (1), which describes the coefficient of absorption for an intensity dependent RSA material, cannot be used in the case of SiNc. This is because the nonlinearity exhibited by SiNc is fluence dependent rather than intensity dependent. Fluence is defined as energy per unit area (J/m^2).[5]

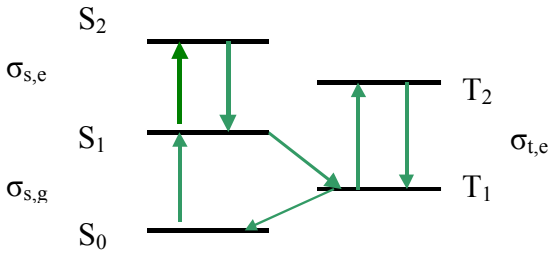

Figure 3 shows a five-level energy model that is used to model reverse-saturable absorption in bulk SiNc.

The five-level model shown in Figure 3 is known to accurately describe the absorptive behavior of bulk SiNc solutions. The electron transitions in such a model occur in the same manner described in the three energy level model used to explain reverse-saturable absorption (RSA). However, a five-level energy model describes a system in which electrons are able to make transitions between five energy levels instead of only three. Here, S represents the system's available singlet energy levels and T represents available triplet energy levels.[7] Experimentation has shown that SiNc's singlet ground state cross-section, σ_g, is 2.3 X 10^{-18} cm^2, while the single excited state cross-section, $\sigma_{s,e}$, and the triplet state cross-section, $\sigma_{t,e}$, are found to be 33.4 X 10^{-18} cm^2 and 112 X 10^{-18} cm^2 respectively.[8] These values indicate that SiNc is a reverse-saturable absorber. However, it should be noted that, in this material, the majority of the absorption processes that lead to absorptive nonlinearity occur in the transition to the second triplet state (T_2).

C. Specimen Apparatus

As previously discussed, nonlinear materials, such as SiNc, are useful when combined with waveguide systems. The cores of these waveguides will be filled with SiNc and will thus exhibit optical limiting over the light's propagation path. Thus, it is important to understand the principles that govern the propagation of light in a waveguide.

1. Total Internal Reflection

Light refracts when it propagates from one medium to another medium with a different index of refraction, as shown if Figure 4. When light enters a medium with a lower index of refraction, the light bends away from the surface normal. The opposite is true for light entering a medium with a higher index of refraction. The relationship between index of refraction and angle (with respect to the surface's normal) is given in Snell's Law as:

$$n_1 \sin\theta_1 = n_2 \sin\theta_2 \qquad (8)$$

and is illustrated below in Figure 4.

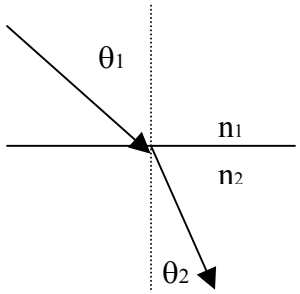

Figure 4 illustrates light refracting at the interface of two indexes of refraction. In this case $n_2 > n_1$ and the light refracts towards the surface normal.

2. Total Internal Reflection in Waveguide Systems

Waveguides are based on the optical principle of total internal reflection (TIR), a direct consequence of Snell's Law. For TIR to occur, light must be propagating towards a medium with an index of refraction lower than that of the medium from which it is originating. When the incident angle of the light is greater than the critical angle (given by $\sin\theta_c = n_2/n_1$), no light will be refracted into the second medium. Instead, all the light will be reflected back into the first medium.[3]

Waveguide systems are designed to utilize TIR to transmit light over long distances. As shown in Figure 5, the waveguides that will be used in this study consist of two parts: a thick cladding and a central core. The cladding must have a lower index of refraction than that of the core in order for total internal reflection to occur. When this is the case, a waveguide will trap light within its core when light enters the core at a suitable angle. For TIR to occur within a waveguide, the light must enter the core at an angle less than $\theta_{0,max}$ which is given mathematically as[5]:

$$\sin\theta_{0,max}=(n_1^2-n_2^2)^{1/2} \quad (9)$$

This situation is diagramed below:

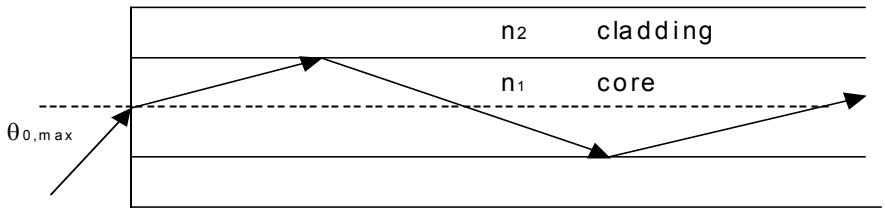

Figure 5 depicts light propagating through the core of a waveguide. This propagation occurs as a result of Total Internal Reflection (TIR).

D. Modal Theory for Circular Waveguides

A mode, in this context of a circular waveguide, refers to a distribution of light's electric field that is able to propagate through the waveguide core. The allowed modes in a waveguide are analogous to standing wave patterns. The first three modes are shown below in Figure 6. Modes are named in accordance with the number of field zeros they have within the core of the capillary. The mode on the far left is thus referred to as the TE_0 mode, the central mode is the TE_1 mode, and the far right is the TE_2 mode.[9]

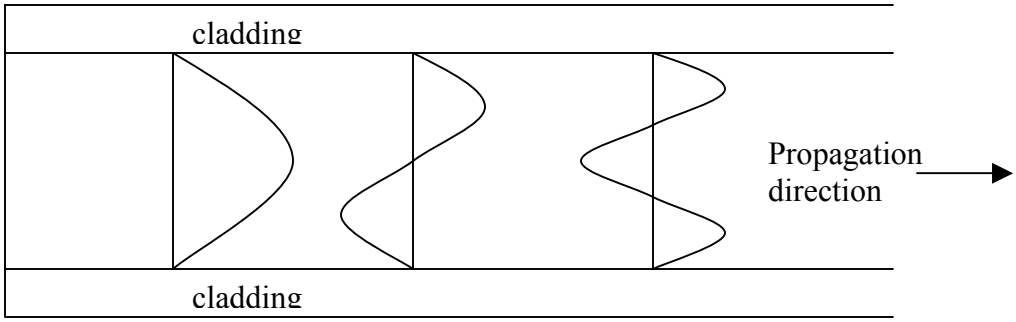

Figure 6 illustrates modes that propagate in a circular waveguide. These modes are named for their number of field zeros. From left to right: TE_0 mode, TE_1 mode, and TE_2 mode.

The manner in which modes of light's electric field propagate through a waveguide is best described by subjecting solutions of Maxwell's equations to the boundary conditions of the waveguide's core-cladding interface. This treatment reveals that only a finite number of modes can be guided through the core of a circular waveguide. Additionally, the solution to this boundary problem reveals that a portion of the guided mode distribution extends in the cladding of the waveguide. This is referred to as the *evanescent field*.[9]

Maxwell's equations relate the electric and magnetic fields associated with light. These equations are listed below in equations 10 through 13.[9]

$$\nabla \times E = -\frac{\partial B}{\partial t} \qquad (10)$$

$$\nabla \times H = \frac{\partial D}{\partial t} \qquad (11)$$

$$\nabla \bullet D = 0 \qquad (12)$$

$$\nabla \bullet B = 0 \qquad (13)$$

In these equations D=εE and B=μH, where ε is the permittivity and μ is the permeability of the medium.[9] In this the project, the medium is the SiNc solution that fills the core of the capillary.

Manipulation of Maxwell's equations reveals equation 14 shown below.[9]

$$\nabla \times (\nabla \times E) = -\mu \frac{\partial}{\partial t}(\nabla \times H) = -\varepsilon\mu \frac{\partial^2 E}{\partial t^2} \qquad (14)$$

A vector identity can be used to transform the left hand side of the equation 14 to the form[9]:

$$\nabla \times (\nabla \times E) = \nabla(\nabla \bullet E) - \nabla^2 E \qquad (15)$$

This leads to the standard wave equations[9]:

$$\nabla^2 E = \varepsilon\mu \frac{\partial^2 E}{\partial t^2} \qquad (16)$$

$$\nabla^2 H = \varepsilon\mu \frac{\partial^2 H}{\partial t^2} \qquad (17)$$

In the case of a circular waveguide, it is best to express the electromagnetic waves propagating in the core in terms of cylindrical coordinates. The direction in which the modes propagate is generally termed the z-direction. The r-direction extends from the center of the waveguide core in the direction of the core radius and the φ-direction is the core's azimuthal direction. This is shown in equation form below[9]:

$$E = E_0(r,\phi)e^{j(\omega t - \beta z)} \qquad (18)$$

$$H = H_0(r,\phi)e^{j(\omega t - \beta z)} \qquad (19)$$

These equations are harmonic in t (time) and z (the direction of propagation). β is the z-component of the propagation vector and is determined by the boundary conditions at the interface of the core and the cladding.

When Maxwell's curl equations are combined with equations 18 and 19 and E_z and H_z are known, the remaining traverse components can be determined.[9]

$$E_r = -\frac{j}{q^2}(\beta\frac{\partial E_z}{\partial r} + \frac{\mu\omega}{r}\frac{\partial H_z}{\partial \phi}) \quad (20)$$

$$E_\phi = -\frac{j}{q^2}(\frac{\beta}{r}\frac{\partial E_z}{\partial \phi} - \mu\omega\frac{\partial H_z}{\partial r}) \quad (21)$$

$$H_r = -\frac{j}{q^2}(\beta\frac{\partial H_z}{\partial r} - \frac{\omega\varepsilon}{r}\frac{\partial E_z}{\partial \phi}) \quad (22)$$

$$H_\phi = -\frac{j}{q^2}(\frac{\beta}{r}\frac{\partial H_z}{\partial \phi} + \omega\varepsilon\frac{\partial E_z}{\partial r}) \quad (23)$$

where $q^2=\omega^2\varepsilon\mu-\beta^2=k^2-\beta^2$.[9]

This treatment reveals the wave equations in cylindrical coordinates.[9]

$$\frac{\partial^2 E_z}{\partial r^2} + \frac{1}{r}\frac{\partial E_z}{\partial r} + \frac{1}{r^2}\frac{\partial^2 E_z}{\partial \phi^2} + q^2 E_z = 0 \quad (24)$$

$$\frac{\partial^2 H_z}{\partial r^2} + \frac{1}{r}\frac{\partial H_z}{\partial r} + \frac{1}{r^2}\frac{\partial^2 H_z}{\partial \phi^2} + q^2 H_z = 0 \quad (25)$$

By separating variables, the guided modes in a capillary core can be found. We adopt a separable form for the solution[9]:

$$E_z = AF_1(r)F_2(\phi)F_3(z)F_4(t) \quad (26)$$

This form can be simplified when one identifies the following relationships.[9]

$$F_3(z)F_4(t) = e^{j(\omega t-\beta z)} \quad (27)$$

$$F_2(\phi) = e^{j\nu\phi} \quad (28)$$

When equation 28 is substituted into equation 26, the wave equation for E_z can be rewritten as shown below[9]:

$$\frac{\partial^2 F_1}{\partial r^2} + \frac{1}{r}\frac{\partial F_1}{\partial r} + (q^2 - \frac{\nu^2}{r^2})F_1 = 0 \qquad (29)$$

An identical equation can be written for H_z. The solutions to these differential equations are known as Bessel functions. These Bessel functions describe the electric and magnetic fields propagating through a waveguide.[5] However, different Bessel functions model the behavior of light inside and outside the core of capillary.

Inside the core, the solutions for the allowed mode profiles must remain finite. These solutions are shown below (*r* denotes the distance from the center of the capillary core, while *a* represents the radius of that core).[9]

$$E_z(r < a) = AJ_\nu(ur)e^{j\nu\phi}e^{j(\omega t - \beta z)} \qquad (30)$$

$$H_z(r < a) = BJ_\nu(ur)e^{j\nu\phi}e^{j(\omega t - \beta z)} \qquad (31)$$

Examples of the zero, first, and second order Bessel functions that propagate in the core are plotted below:

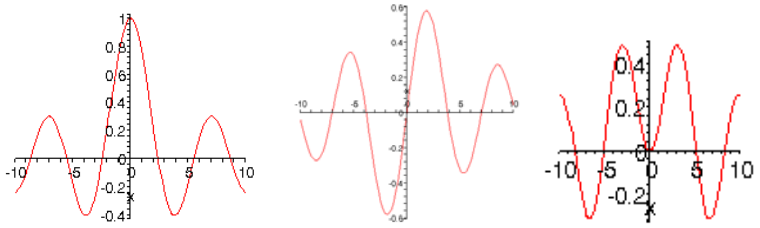

Figure 7 shows (from left to right) the zero, first, and second order Bessel Function of the first kind that represent the modes that propagate through a waveguide core.

Outside the core, the cladding of the waveguide is modeled as extending to infinity. As a result, the solution for a given mode decays to zero as the distance from the center of the waveguide core proceeds to infinity. These solutions are represented below[9]

$$E_z(r > a) = CK_\nu(wr)e^{j\nu\phi}e^{j(\omega t - \beta z)} \qquad (32)$$

$$H_z(r > a) = DK_\nu(wr)e^{j\nu\phi}e^{j(\omega t - \beta z)} \qquad (33)$$

A, B, C, and D are arbitrary constants in the four equations stated above. Examples of the zero, first, and second order Bessel functions that decay in the cladding are plotted below:

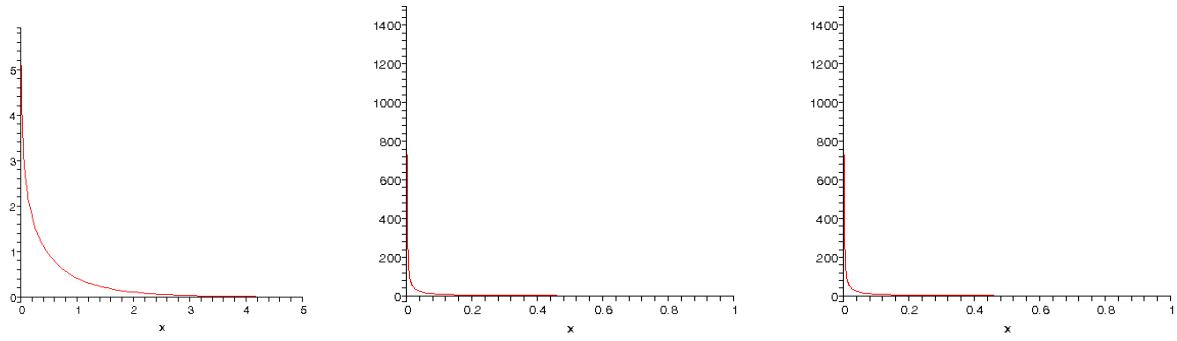

Figure 8 shows (from left to right) the zero, first, and second order Bessel Function of the second kind that represent the modes that decay in the waveguide cladding.

The tangential components of light's electric field, E_z and E_φ, and the tangential components of light's magnetic field, H_z and H_φ, must be continuous at the interface of the waveguide's core and cladding. By matching the Bessel functions that describe modes propagating in the core and those that describe the evanescent field that decays in the cladding, one can solve for the arbitrary constants A, B, C, and D in equations 30 through 33. This reveals that there are only solutions for these coefficients for discrete values of β. The fact that one mode corresponds to one value of β, enables one to find the number of modes that propagate in a waveguide core by solving this boundary condition problem.[5]

As the difference in index of refraction between the waveguide's core and cladding decreases, fewer modes are allowed to propagate in the waveguide core. When this difference is less than 1 percent, the set of allowed modes is called the linearly polarized modes. Solving the boundary conditions of this set leads to a transcendental equation that can be solved for the propagation constants of the allowed modes. This equation is[5]:

$$\frac{uJ_{j-1}(ua)}{J_j(ua)} = -\frac{-wK_{j-1}(wa)}{K_{j-1}(wa)} \qquad (34)$$

In this equation j=ν-1. The number of roots to this equation is equal to the number of modes that can propagate through the waveguide core.[5]

The quantity of allowed modes also depends on a factor known as the V-number given by[5]:

$$V = \frac{2\pi a}{\lambda}\sqrt{n_1^{\,2} - n_2^{\,2}} \qquad (35)$$

In most cases, as the V-number increases, the waveguide allows more modes to propagate. Thus, as waveguide cores get larger (with respect to the wavelength of light) more modes are supported.[5]

Under certain conditions, waveguides will only allow one mode (the TE_0 or fundamental mode) to propagate. For this to occur the fiber's core diameter must be on the order of a couple of wavelengths of light and the difference in index of refraction between the core and the cladding must be very small (on the order of 10^{-4}).[9]

3. Test Apparatus

In order to study optical limiting in a SiNc filled waveguide, an apparatus must be constructed to make coupling laser light into the capillary core experimentally feasible. ENS J.J. Wathen designed such an apparatus during the fall semester of the 2001-2002 academic year in order to study optical limiting in multi-mode waveguide systems. The purpose of the apparatus is to hold a filled capillary between input and output microscope objectives. Light must propagate through the input objective and then be coupled into the waveguide. This light will propagate through the core via total internal reflection (TIR). Upon exiting the core, this light will enter the output microscope objective and be imaged at a certain distance along the propagation axis (convention often refers to this as the z-axis). The waveguide portion of this apparatus is illustrated below in Figure 9.

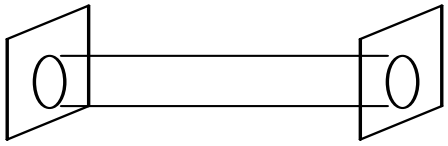

Figure 9 is an illustration of a waveguide suspended between two optical flats.

This illustration shows a waveguide suspended between two optical flats. These flats must be coated with the same fluid that is in the core of the waveguide. This coating fluid prevents a meniscus from forming at the intersection of the waveguide and the optical flat. This allows light to be coupled into and out of the waveguide without being interrupted by the refraction that would occur if that light were to propagate through an air filled meniscus. The optical flats and

the waveguide are supported by a structure consisting of microscope slides and a metal waveguide support block.

4. Experimental Setup

Developing, implementing, and modifying an experimental set-up conducive to data collection of optical limiting in a single-mode waveguide system has constituted a significant amount of work done during this Trident project. The set-up that will be used for data collection is shown below. The individual components are discussed in the following subsections.

Figure 10

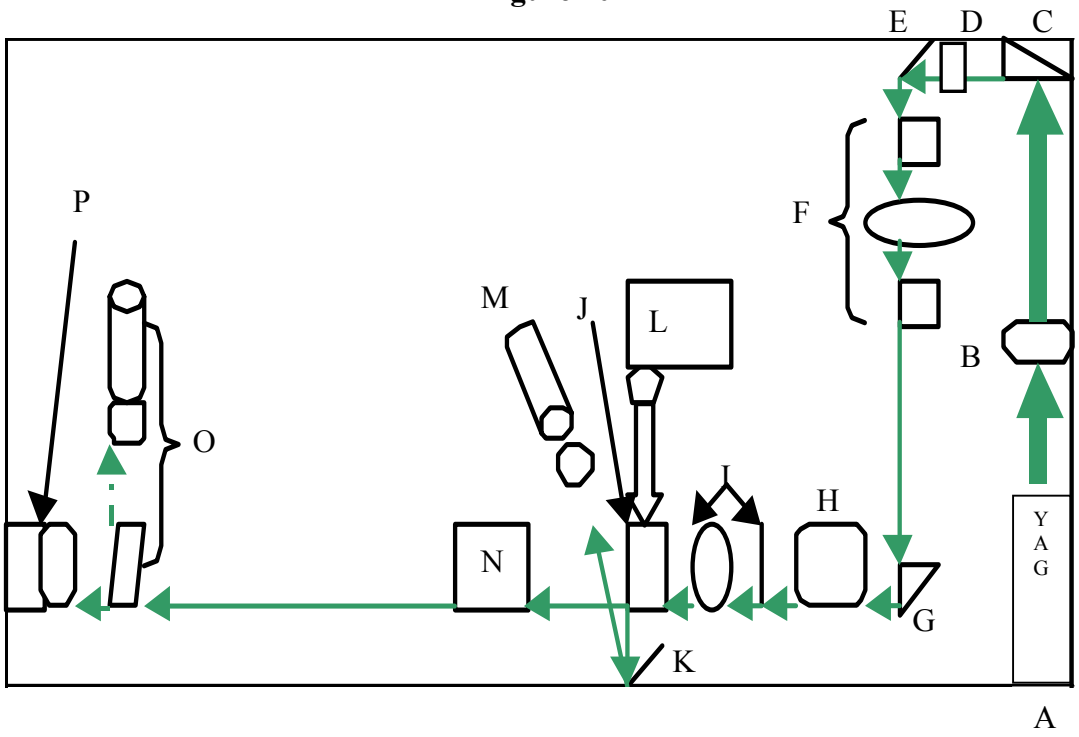

A: 532 nm frequency-doubled YAG laser
B: Beam elevating mirrors
C: Prism
D: Parallel Plate Attenuator
E: Mirror
F: Polarizing beam cube, birefringent liquid crystal, and analyzing beam cube
G: Prism
H: Spatial Filter
I: Iris and Beam Collimator
J: Pick-off wedge
K: Mirror
L: While Light Source
M: Input energy probe and Filter Wheel
N: Input microscope objective, Specimen Apparatus, Output Microscope Objective, and Heater
O: Three point stand (holding mirror), Filter wheel, and Output Microscope Objective
P: Filter Wheel and Imaging Camera

A. 532 nm Frequency-Double YAG Laser

The laser being used in this experiment was produced by Brilliant Corporation and produces 4ns pulses of light at a wavelength of 532 nm (green). This laser has the ability to produce high-energy pulses and is thus similar to the types of lasers that may eventually be used as weapons.

B. Beam Elevating Mirrors

The beam elevating apparatus consists of two mirrors oriented in a manner that enables them to raise the emitted laser beam from the height of the laser's head to a height at which optical equipment can be more easily placed. This set-up is illustrated below.

Figure 11

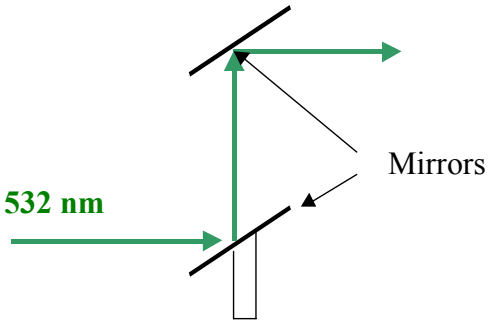

Figure 11 depicts two mirrors oriented in such a way that they raise an incoming laser beam to a height convenient for the implementation of optical equipment.

C. Prism

After being elevated by the mirror apparatus described above, the raised beam proceeds to a prism. This prism directs approximately four percent of the incident beam towards the rest of the optical set-up and directs all remaining energy to one of two beam blocks (not shown in diagram) where that energy is absorbed. This is an important feature because it lowers the main

beam's energy level to a point that is within the parameters of the optical equipment that will be used to collect data (i.e. sensors and imaging camera).

D. Parallel Plate Attenuator

This device contains plates of a material that has a reflectivity that is dependent on the angle of light incident upon them. The angle of these plates, and thus the amount of light they reflect, is controlled be a dial located on the exterior of the device. This dial allows the operator to control the amount of attenuation experienced by the laser beam passing through the attenuator.

E. Mirror

This mirror is specially designed to reflect 532 nm light. The purpose of this device is simply to redirect the beam towards the rest of the optical set-up with virtually no energy loss.

F. Polarizing beam cube, birefringent liquid crystal, and analyzing beam cube

This portion of the experimental setup consists of two polarizing beam cubes that are oriented 90 degrees to one another. By themselves, these cubes would eliminate all light from the propagation path (one linear polarization is eliminated at the initial beam cube and the opposite polarization at the second beam cube). However, we have placed a liquid crystal variable retarder between these cubes. This device alters the linear polarization that is induced by the first cube, allowing a portion of the light to pass through the second beam cube. The variable retarder is connected to a control device that alters the crystal's polarization properties. By changing the manner in which the liquid crystal repolarizes the input light, varying amounts light can be transmitted to the remainder of the experimental set-up. As a result, the polarizing beam cubes and the variable retarder provide a means to control the input intensity to the waveguide being studied.

G. Prism

The second prism in this set-up redirects the beam towards the specimen apparatus. Unlike the prism encountered earlier in the set-up, the faces of this prism are oriented to the incoming beam in such a manner that approximately 90 percent of the beam is sent towards the test specimen.

H. Spatial Filter

The purpose of the spatial filter is to eliminate imperfections in the beam profile and ensure that the beam distribution is nearly Guassian. This is accomplished as the beam is focused through the high-energy pinhole portion of the device. This pinhole has a diameter of 10 μm.

I. Iris and Beam Collimator

The spatial filter is followed by an iris, which allows the width the incoming beam to be controlled. After the iris has altered the beam width to a desired size, the beam passes through a large lens called a *beam collimator*. This lens counteracts divergence as the beam travels down the remainder of the propagation axis.

J. Pick-off wedge

An optical wedge was used to pick off approximately 3.33 percent of the main beam and reflect it to a mirror. The remainder of the main beam continues along the propagation axis.

K. Mirror

A mirror was positioned to redirect the pick-off beam, which was reflected from the optical wedge, towards the input energy sensor.

L. White Light Source

The white light source sends white light to the set-up's third polarizing beam cube, which redirects that light towards the test apparatus. As previously mentioned, this allows the experimenter to form a clear image of the waveguide core at some distance along the propagation axis.

M. Input Energy Probe and Filter Wheel

After a portion of the main laser beam is redirected by the third polarizing beam cube and then reflected off a mirror, it is measured by the input energy probe. The relationship between the main beam and this picked off portion of the beam allows the experimenter to use the measured energy value of the picked off beam to determined the amount of energy entering the waveguide system. The energy probe can be damaged if exposed to energies exceeding 20 nJ. As a result, a filter wheel that can absorb varying amounts of input energy protects the probe.

N. Input Microscope Objective, Specimen Apparatus, Output Microscope Objective, and Heater

The purpose of the input microscope objective is to focus light into the core of the waveguide being studied. The specimen apparatus holds the waveguide between the objectives and is supported by a heating platform. This heating device allows the experimenter to tune the indices of refraction between the waveguide core and cladding through thermal expansion. In order for a waveguide to exhibit single-mode behavior, this index of refraction difference must be on the order of 10^{-4}. After the light exits the core of the waveguide, it is brought into focus at some point along the propagation axis by the output microscope objective.

O. Three-point stand (holding mirror), Filter wheel, and Output Optical Sensor

Towards the far end of the optical table (with respect to the initial portion of the experimental set-up), is a three-point stand that allows the experimenter to move a mirror into and out of the experimental set-up with ease. When in place, this mirror redirects the main beam towards an output optical sensor, where the energy of the beam leaving the waveguide is measured. This sensor can be damaged if the input signal exceeds 20 nJ. Thus, a filter wheel is placed in front of the sensor. The filter wheel can be set to absorb varying percentages of light.

P. Filter Wheel and Imaging Camera

As previously discussed, the output microscope objective images the light exiting the core of the waveguide at some distance along the propagation axis. When forming this image, it is important to ensure that the end of the waveguide is located as close to the output objective's focal point as possible. This causes the core to be imaged at a great distance from the objective and produces the greatest magnification.

When the mirror is removed from the three-point stand discussed above, the light propagates to a beam-imaging camera developed by Coherent Corporation. This camera allows the experimenter to view on a computer monitor the image created by the light exiting the waveguide core. This is accomplished through data analysis software called Beam View. In addition, this software represents intensity variations in the beam profile by correlating intensity at a given point with a certain color.

5. Methodology

After the test apparatus is constructed, it is placed upon a heating plate located between the input and output objectives. Micrometers allow the operator to adjust the distance of the microscope objectives from the ends of the capillary. The input objective must be set so that the front end of the capillary is near the focal length of the objective. This allows for a maximum amount of light to be focused into the core of the waveguide. The output objective must be set approximately one focal length away from the end of the capillary. This provides an image of the waveguide core with the greatest magnification possible.

Pulses of laser light (532 nm) were guided through the experimental setup towards the capillary. Micrometers on the stage holding the test apparatus were then used to move the capillary until a maximum amount of light is coupled into the core.

Once this maximum coupling was achieved, the heater was used to tune the index of refraction of the core and cladding. The temperature at the location of the capillary was determined by a thermistor located on the metal block that holds the waveguide. Adding heat to the test apparatus causes the index of refraction of the core to decrease as the liquid expands. The change in index of refraction of the core was expected to be at least an order of magnitude larger than that of the solid glass cladding. The change in index of refraction of the core and the cladding leads to a smaller difference in the indices of refraction and eventually allows the waveguide to become single-mode.

After the test apparatus reaches thermal equilibrium for a desired heater temperature and coupling efficiency into the waveguide core has been maximized, the mode profile must be observed and analyzed. This was accomplished by observing the image of the end of the

capillary on a digital camera. This image seen by the camera was displayed on a computer monitor where varying intensities are shown in different colors. It is this image that allows the experimenter to determine whether the applied heat has caused the waveguide to become single-mode. The image of a single-mode waveguide will exhibit a Gaussian looking energy profile that fades in and out, but remains fixed in shape when the test holder micrometers are used to alter the coupling efficiency into the core. Conversely, the image of a multi-mode waveguide does not necessarily exhibit a Gaussian looking energy profile and, altering the coupling efficiency into the core, causes the image to become distorted, indicating that different mode structures are being excited. The computer software associated with this camera allows the experimenter to save the image of the mode profile in question.

After obtaining an image of the mode profile, a mirror on a three-point stand is used to redirect the beam towards the output energy sensor. The parallel plate attenuator is then used to vary the input beam energy. A computer program records the energies observed by both the input and output energy sensors, allowing the amount of optical limiting to be determined through data analysis.

6. Computer Modeling of SiNc

A Fortran program was designed by researchers at the Naval Research Laboratory to predict the optical limiting that occurs in various RSA solutions. This program was designed to model optical limiting in a bulk material and does not take the confinement imposed by the capillary into account.[5]

The program simulates light pulses, assumed to be Gaussian in both time and space, entering a nonlinear material. By determining the nonlinear absorption that the material should experience at this input energy, the program generates two columns of data: one for input energy per pulse and one for output energy per pulse.[5]

In order to make these calculations, the program must be given a certain parameters. These include the wavelength of the input light, SiNc's σ_g and σ_e (ground state and excited state cross sections), the waveguide core diameter (R_0), the concentration of SiNc molecules (C_0), the waveguide length (L_0), the full-width-half-maximum pulsewidth (Tfwhm), and the initial pulse energy (E_0).[5]

Using this information, the program calculates the material's transmission by making the assumption that all the SiNc's molecules start in their ground state. This is accomplished by calculating the coefficient of absorption when all the SiNc molecules are unexcited. This calculation is made using σ_g, the SiNc ground state absorption cross section, and C_0, the solution's molar concentration, in equation 36 below[5]

$$\alpha = \alpha_g = \sigma_g C_0 N_A \frac{1L}{1000mL} \qquad (36)$$

where N_A is Avogadro's Number. The program then calculates the sample's linear transmittance using this coefficient of absorption, α, and the length of the material, L_0. This relationship is shown below.

$$T_{linear} = e^{-\alpha L_0} \qquad (37)$$

The simulation then generates a simulated input pulse. The previously mentioned full-width-half-maximum pulse width is used for the simulated pulse's temporal width while the waveguides core diameter serves as the pulse's spatial width. The simulation then sends this pulse thought the simulated waveguide core.

The program has the ability to then make transmission calculations at a given time. At a give time, each section of the core will be interacting with a different number of photons. This variation is due to the fact that the pulse is assigned a Gaussian energy distribution. Consequently, the greater the number of photons in a given differential volume of the core, the greater the number of photons that can be absorbed in that differential volume. The program calculates the number of photons, G, that can be found in a differential volume of the core using the following equation to make this calculation

$$G = \frac{I(r,z,t)}{h\nu} dt \qquad (38)$$

where I(r,z,t) is the pulse intensity at that particular differential volume and dt is the differential time period over which the pulse acts on that differential volume.[5]

The more photons a particular volume of the core absorbs, the more nonlinear molecules reach an exited energy state in that volume. The program calculates the number of molecules that reach this first excited state, G_1, using the following equation

$$G_1 = M_0 \sigma_g G \qquad (39)$$

where M_0 is the original concentration of ground state molecules. The new population of ground-state molecules becomes

$$N_0 = M_0 - G_1 \qquad (40)$$

where N_0 is the ground-state density after time dt. The new population of the first excited state becomes

$$N_1 = M_1 + G_1 \qquad (41)$$

where N_1 is the excited state's density after a time dt and M_1 is the excited state's density at the beginning of time interval dt.[5]

The new coefficient of absorption at a particular differential volume then becomes

$$\alpha_{(r,z,t)} = \sigma_g(N_0) + \sigma_e(N_1) \qquad (42)$$

This newly determined coefficient of absorption is used to determine the number of photons that a differential volume will absorb when the next portion of the pulse acts on it.[5]

The program later integrates the absorption effects over all differential volumes in the core and over all differential time intervals to determine the total amount of energy the nonlinear material in the core absorbs from a given input pulse. Thus, the transmission for a given pulse is

$$T = \frac{E_{in}}{E_{out}} \qquad (43)$$

and relative transmission is

$$T_{rel} = \frac{T}{T_{linear}} \qquad (44)$$

7. Results and Discussion

A. Compiled Data

The collected data was analyzed, allowing a number of interesting behaviors to be observed. In order to interpret this data it was necessary to calculate the input and output energies experienced by the sample and the sample's relative transmission.

To calculate the energy input into the sample, the energy recorded at the input sensor must be properly manipulated. As indicated in the Experimental Setup portion of this report, the input energy sensor measures the energy of a portion of the main beam picked-off by an optical wedge. This wedge picks off approximately 3.33 percent of the main beam. The noise level at the input energy sensor, measured to be 0.03 pJ, must be subtracted from the energy value measured at the input sensor. This value of the picked off beam allows for the determination of the energy value of the main beam. This is achieved by dividing the pick-off beam energy value by the percentage that relates the pick-off and main beams (3.33 percent). The losses that occur as the main beam passes through the input microscope objective and then through the input microscope cover slide must be taken into account. This is accomplished by multiplying by the transmission of the microscope objective (86.43 percent) and by the transmission of the microscope cover slide (96 percent). This value must be multiplied by the coupling efficiency, defined as the percentage of light entering the waveguide. This value will vary with different data runs. The coupling efficiencies associated with the data runs conducted at different temperatures is shown in Table 1 below.

Table 1:

Coupling Efficiencies at Various Temperatures

Temperature (C)	Coupling Efficiency (%)
27.4	36.030
30.0	35.998
52.7	17.288
55.9	17.143
60.8	24.304
64.1	22.094
64.5	17.624
66.5	20.610
69.1	12.318
70.4	4.488

The energy output from the sample can be determined in a similar fashion. An energy value is measured at the output sensor. The noise level at this sensor, measured to be 0.25 pJ, must be subtracted from this value. This value must then be corrected by dividing it by the transmission of the output microscope objective (78.38 percent) and the transmission of the output microscope cover slide (96 percent). This treatment yields a value for the output energy of the sample.

Having calculated the input and output energies, one must now determine the relative transmission of the sample. The transmission is determined by dividing the output energy by the

input energy. This value becomes relative transmission when the transmission value is divided by the linear transmission of the solution in the core. This value was found to be approximately 48.2 percent.

A representation of the findings at different sample temperatures can be seen below in Figure 12. This graph considers all energy included in the propagating mode structure, both the portion of the mode in the waveguide core and the portion in the cladding.

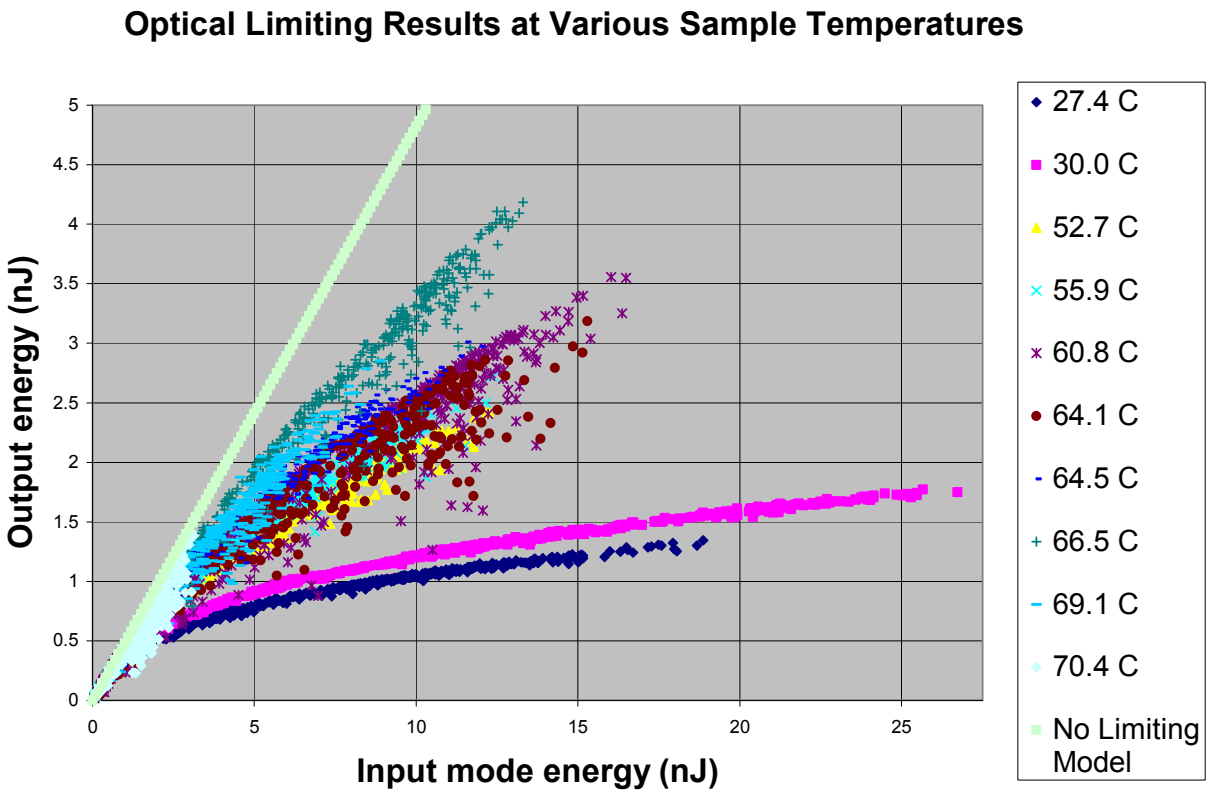

Figure 12 shows output energy graphed as a function of input intensity at different temperatures. This graph shows that optically limiting is enhanced in multi-mode waveguides, where the entire mode is confined to a region within the core.

Figure 12 represents output energy as a function of input energy at a variety of different sample temperatures. The most general conclusion that can be drawn from this data is the

fact that multi-mode waveguides exhibit better optical limiting than single-mode waveguides. This is evident as the multi-mode systems, which exist at 27.4 and 30.0 °C, show lower output energy for a given input energy than the other data series, which are all single-mode systems.

This result is contrary to expectations. It had been assumed single-mode waveguides would exhibit better limiting than their multi-mode counterparts. This expectation was due to the belief that the fundamental mode would confine the beam to a smaller traverse area, enhancing its intensity and thus its optical limiting effect. In addition, it was believed that, as the most intense portion of the mode profile underwent optical limiting, the mode would be forced to reshape itself and light would be lost to the exterior of the waveguide cladding. The fact that this did not come to pass is a surprising result, but can be explained.

This data can also be presented as the relative transmission as a function of input mode energy. Again, input mode energy is defined as all the energy contained within the mode structure, both the portion of the mode in the core and in the cladding. This representation indicates the amount of nonlinear absorption occurring at a given mode structure and is shown below in Figure 13.

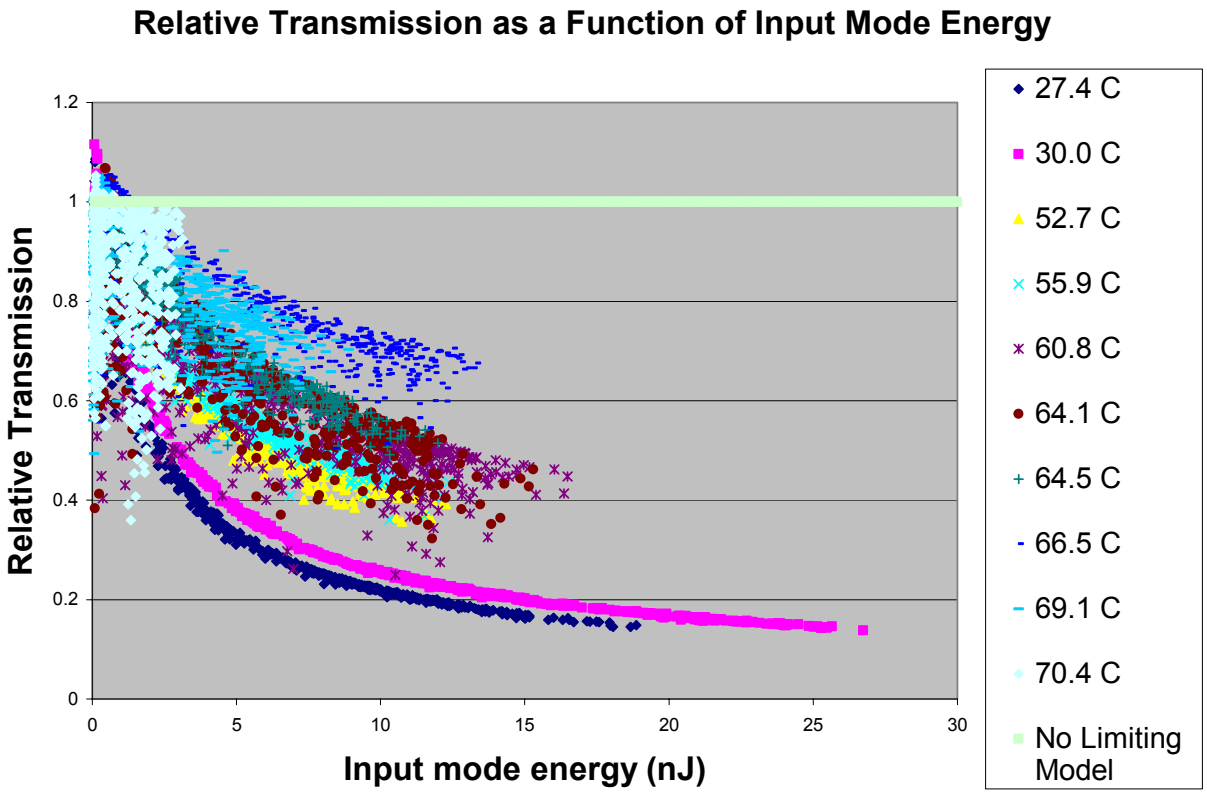

Figure 13 shows relative transmission graphed as a function of input intensity at different temperatures. This graph also shows that optical limiting is enhanced in multi-mode waveguides.

Again, this representation of the data confirms that the multi-mode waveguides exhibit better optical limiting than single-mode waveguides. This is due to the fact that, in a multi-mode system, the entire mode structure is confined within a region of the waveguide core, allowing the optical limiting to occur over the entire mode. In a single-mode waveguide, a portion of the mode extends into the cladding, avoiding the SiNc solution that enacts optical limiting. The data also shows that for single-mode waveguides, as temperature of the sample increases and the difference in index of refraction of the core and cladding decreases, the amount of optical limiting decreases. This is because when the core and the cladding near a match in index of refraction, a greater portion of the mode energy extends into the cladding.

B. Multi-mode results

The multi-mode data taken in this project is consistent with the data taken by ENS Wathen (USNA Class of 2002) in his Trident project, which examined optical limiting exclusively in a multi-mode waveguide. This consistency can be seen in Figure 14 shown below.

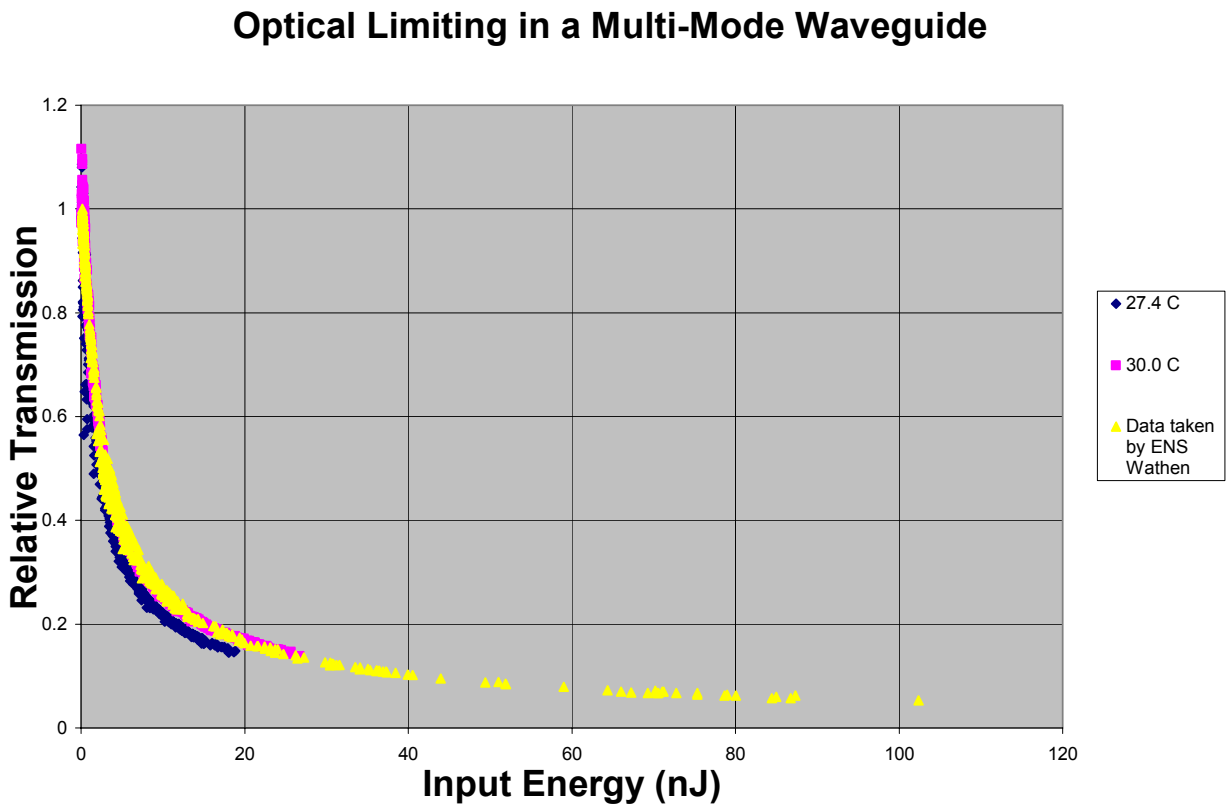

Figure 14 shows relative transmission graphed as a function of input energy into the waveguide. This data is consistent with the multi-mode waveguide data taken by ENS J.J. Wathen in 2002.

It is interesting that these results are so consistent when one considers that the waveguide in ENS Wathen's experiment contained many more modes than the multi-mode systems examined in this study. The approximate number of modes that a particular waveguide can support can be calculated using the following equation[9]

$$M \cong \frac{2\pi^2 a^2}{\lambda^2}(n_1^2 - n_2^2) \cong \frac{V^2}{2} \qquad (45)$$

This equation reveals that the data taken by ENS Wathen's waveguide (3.2 μm diameter core) supports approximately 12 modes, while the multi-mode systems examined in this study (2 μm diameter core) only supported two modes. This difference is due to the larger core and the larger difference in index of refraction between the core and cladding in the waveguide used by ENS Wathen.

White light can be used to image the waveguide core on a digital camera. This method allows the experimenter to correctly position the output microscope objective so that the end of the waveguide core is in focus on the camera. In addition, it is useful to compare a picture of the core imaged with white light to the modal profile imaged when the laser light is coupled into the core. A white light image of the core is shown below.

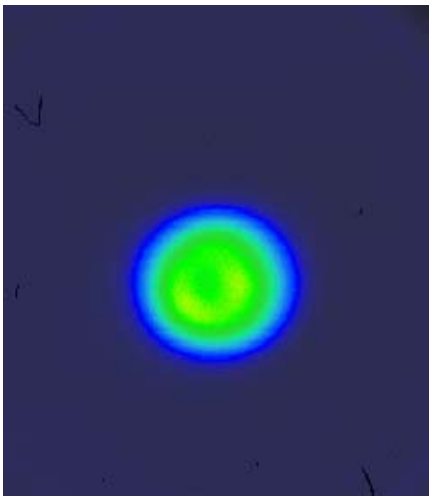

Figure 15 shows the core imaged with white light.

The mode profile in a multi-mode waveguide has multiple lobes, indicating various excited modes. The mode profile associated with a sample temperature of 30.0° C is shown below in Figure 16.

Figure 16 shows the mode profile for a multi-mode waveguide system. The lobes represent various excited modes in the waveguide core.

It is also interesting to examine how the multi-mode data fits with a theoretical model. This data fit was accomplished using a computer program. In this program, the effective beam diameter is left as the free parameter. Varying this value allows the program operator to match the data to a theoretical model. These individual fits are shown below in Figures 17 and 18.

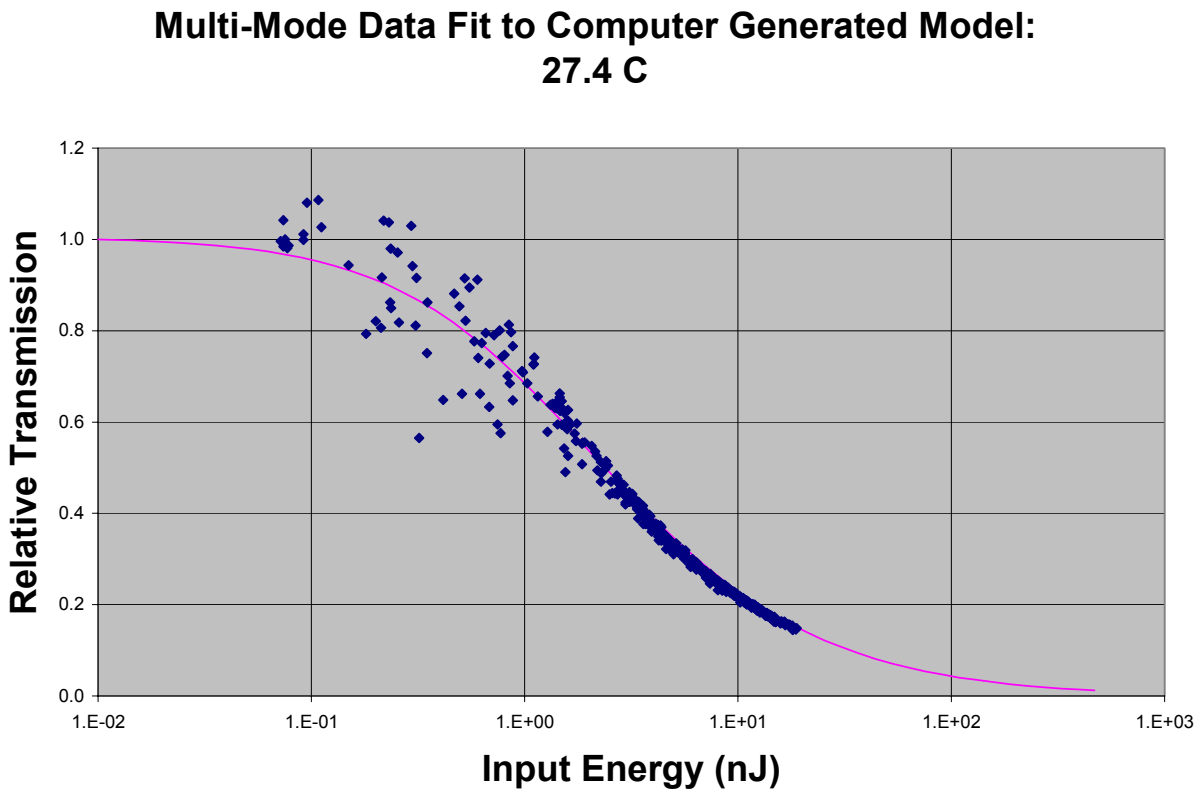

Figure 17 shows the multi-mode data at 27.4 C. This data is fit to a theoretical model using the Fortran model.

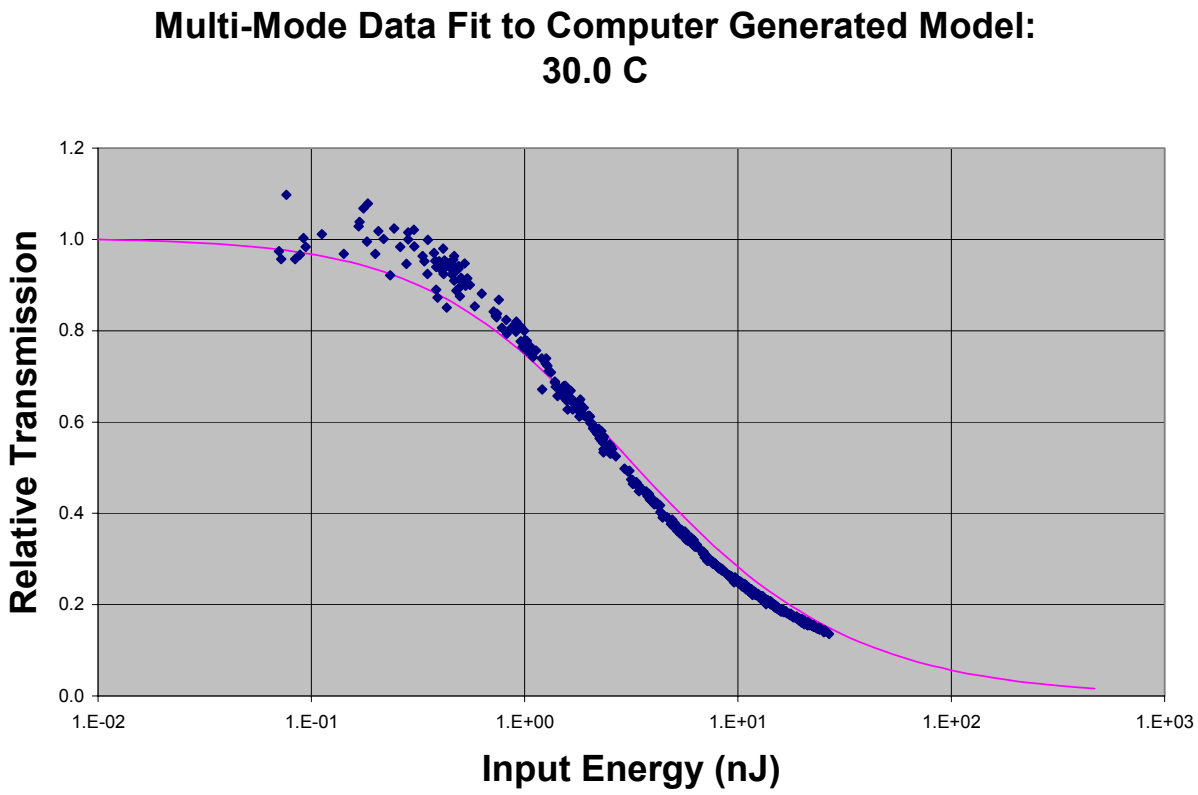

Figure 18 shows the multi-mode data at 30.0 C. This data is fit to a theoretical model using a computer generated model.

These models predict a 1.6 μm effective beam diameter at 27.4 °C and a 1.9 μm effective beam diameter at 30.0 °C. This is consistent with other examinations of multi-mode waveguides. It was found in a previous study, conducted by ENS Wathen (USNA 2002) that, in a multi-mode waveguide, the entire mode structure is confined to a region within the core. This enhances the optical limiting effect.

The Fortran program shows that the effective beam diameter increases as increased sample temperature decreases the difference in index of refraction between the waveguide core and cladding.

C. Single-mode results

As the sample temperature increases, the waveguide becomes single-mode at approximately 52.7 °C. This was determined by examining the mode profile at that temperature. The mode profile at 52.7 °C is shown below in Figure 19.

Figure 19

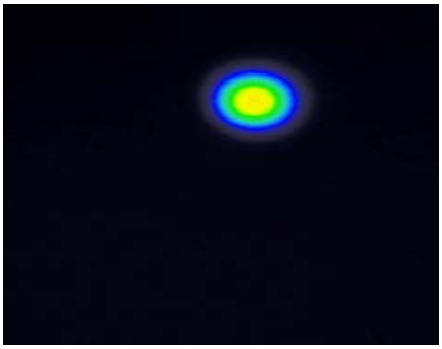

Figure 19 shows a single-mode profile.

When single-mode, the mode profile appears as a Gaussian looking spot. This spot fades in and out, but does not distort itself as the coupling efficiency is altered. The fact that the spot cannot be distorted is indicative of the fact that, once a waveguide has met single-mode conditions, other modes cannot be excited in it.

Single-mode data can also be fit to theory using a computer program. This fit for 52.7 °C is shown in Figure 20.

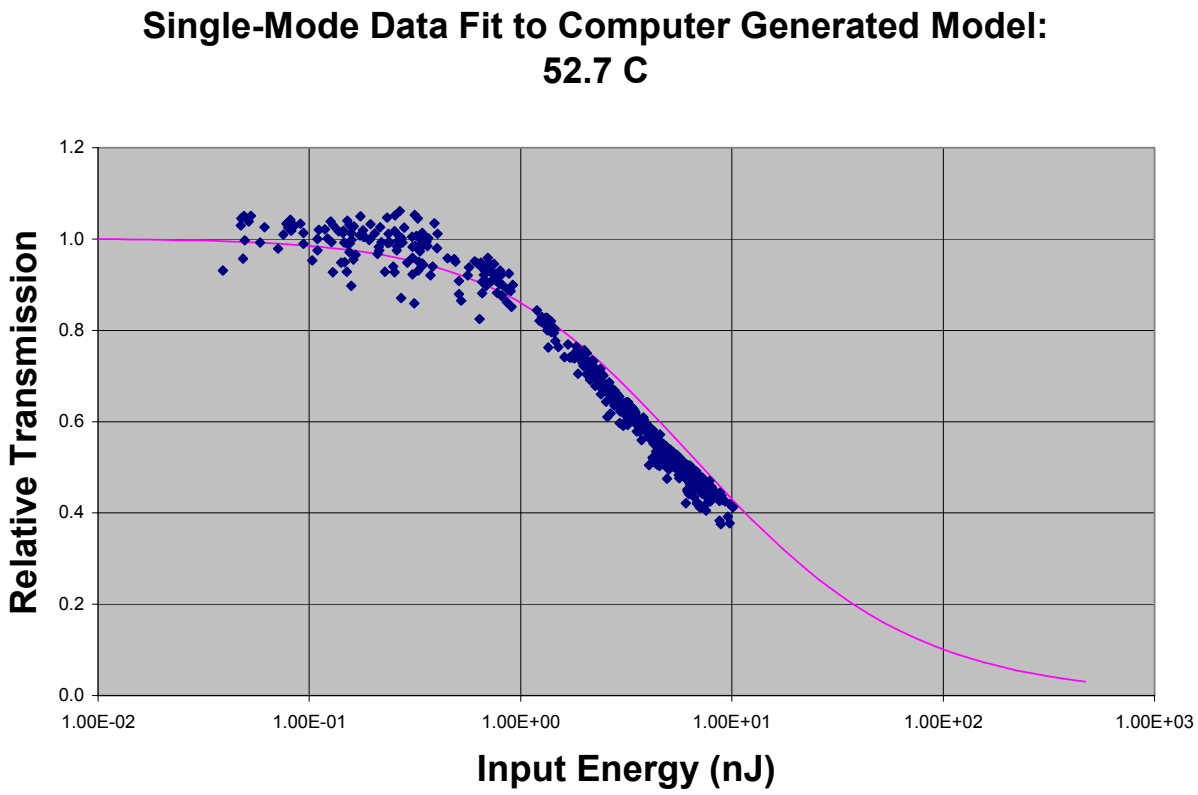

Figure 20 shows the single mode data at 52.7 C. This data is fit to a theoretical model using a computer generated model.

The Fortran program finds the effective beam diameter to be 2.8 μm. However, it is important to note that the Fortran program works under the mistaken assumption that the entire mode is confined to the waveguide core. Thus, this information means that this capillary with a 2 μm diameter core at this single-mode temperature shows the same amount of limiting as a waveguide with the entire mode structure confined to a 2.8 μm diameter core.

A Mathcad program allows for a model of the Bessel functions that comprise the mode structure to be formed. In this model, the portion of the mode in the core is shown in red, while the portion in the cladding is shown in blue. A model for the mode structure at 52.7 °C is shown below.

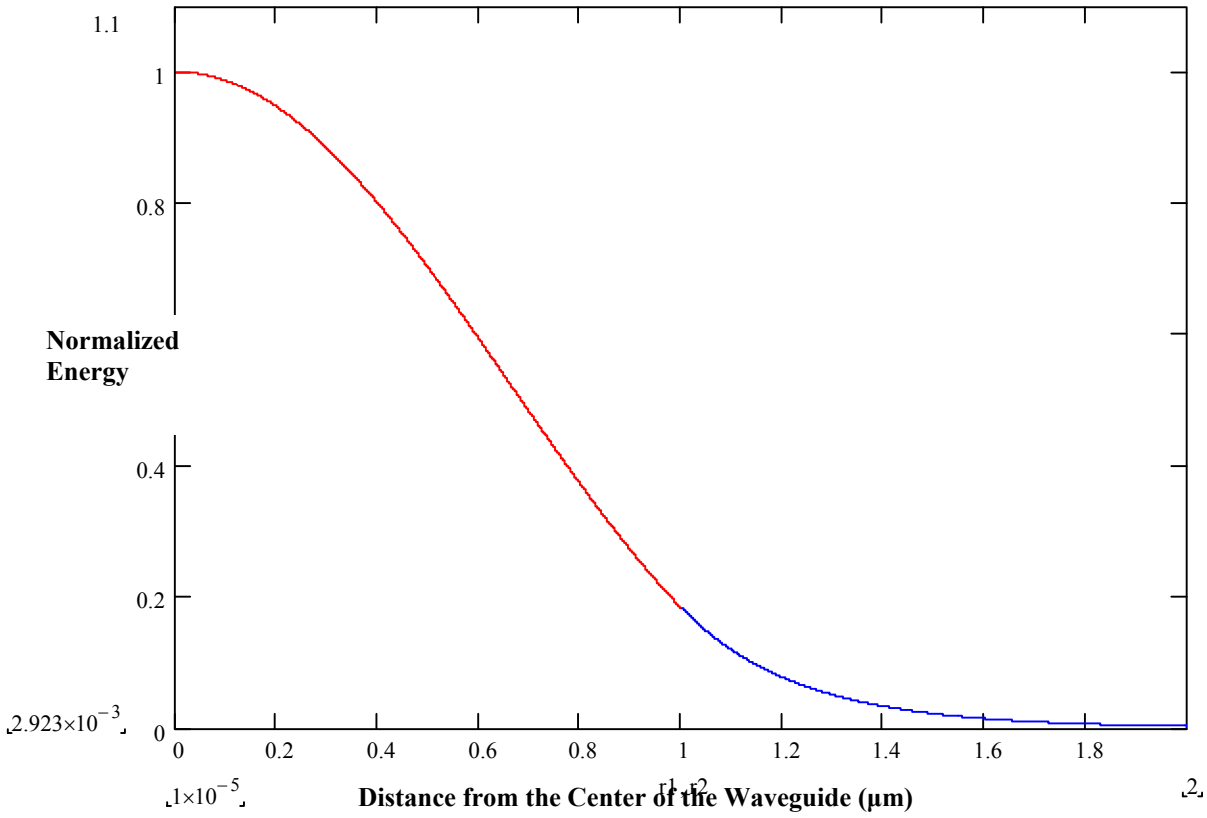

Figure 21 shows a model of the mode profile at 52.7 °C. The red portion is contained in the core and the blue portion is found in the cladding.

This program tells us that, at this temperature, 82.1488 percent of the mode's energy is in the core of the waveguide.

In order to generate this model, the program requires that the operator input the index of refraction of the waveguide core, information that is dependent on the temperature of the sample. This information was achieved by making three assumptions. These assumptions were that the sample became single-mode occurs at a sample temperature of 52.7 °C, that the core and the cladding became index matched at a sample temperature of 70.4 °C, and that index of refraction decreases linearly with increasing temperature.

This process of data analysis can also be applied to other single-mode temperatures and comparisons drawn. The mode profile at a temperature of 60.8 °C is shown in Figure 22.

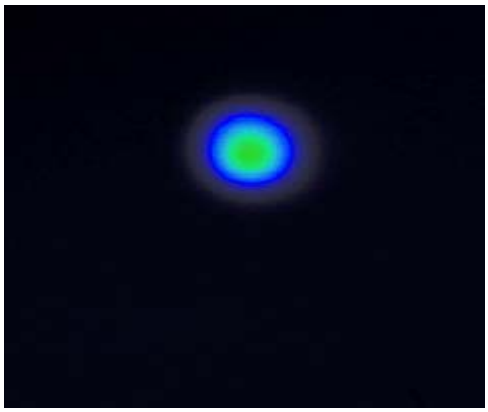

Figure 22 shows the mode profile at the single-mode temperature of 60.8 °C.

The data fit to the computer generated model at this temperature is shown below in Figure 23.

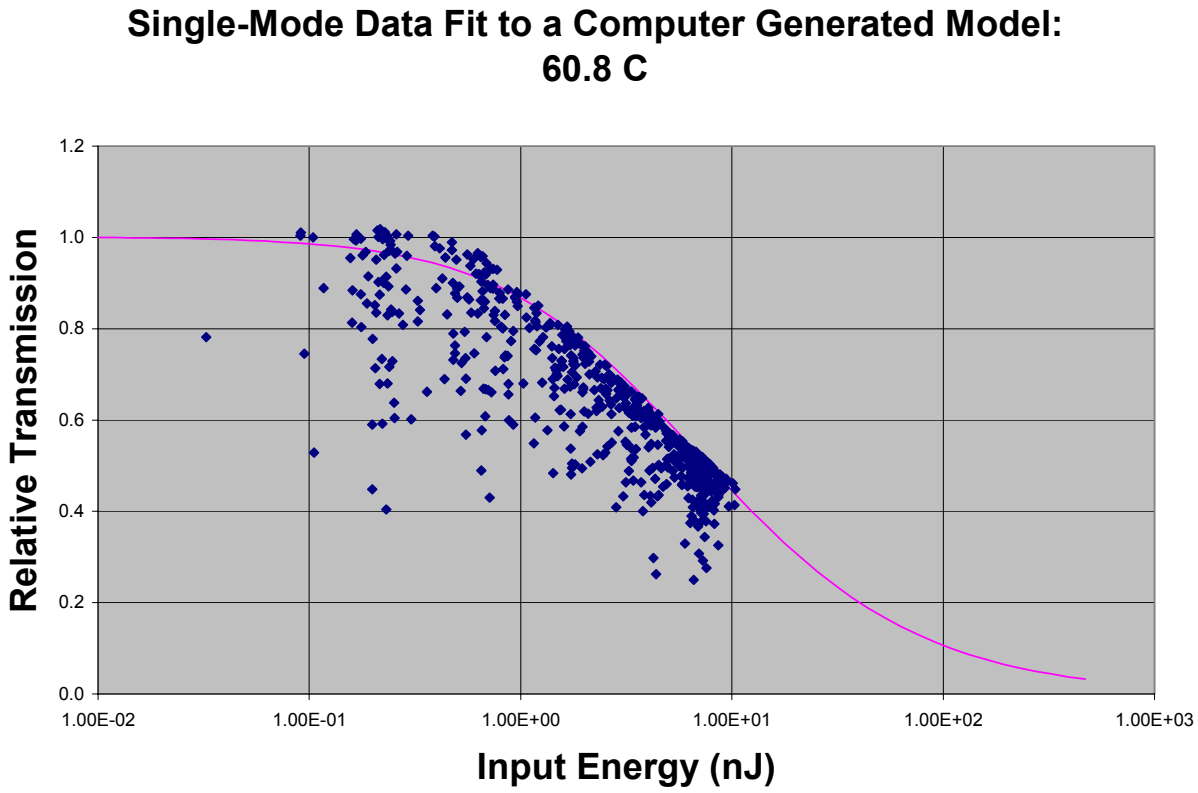

Figure 23 shows the single mode data at 60.8 C. This data is fit to a theoretical model using the Fortran model.

The effective beam diameter at this temperature is 2.9 μm. This tells us that, as temperature increases, the single-mode waveguide shows a slight decrease in its ability to limit.

Again the Mathcad program was used to model the mode profile at this temperature and determine the amount of energy in the waveguide core according to that model. Figure 25 shows the mode profile at 60.8 °C.

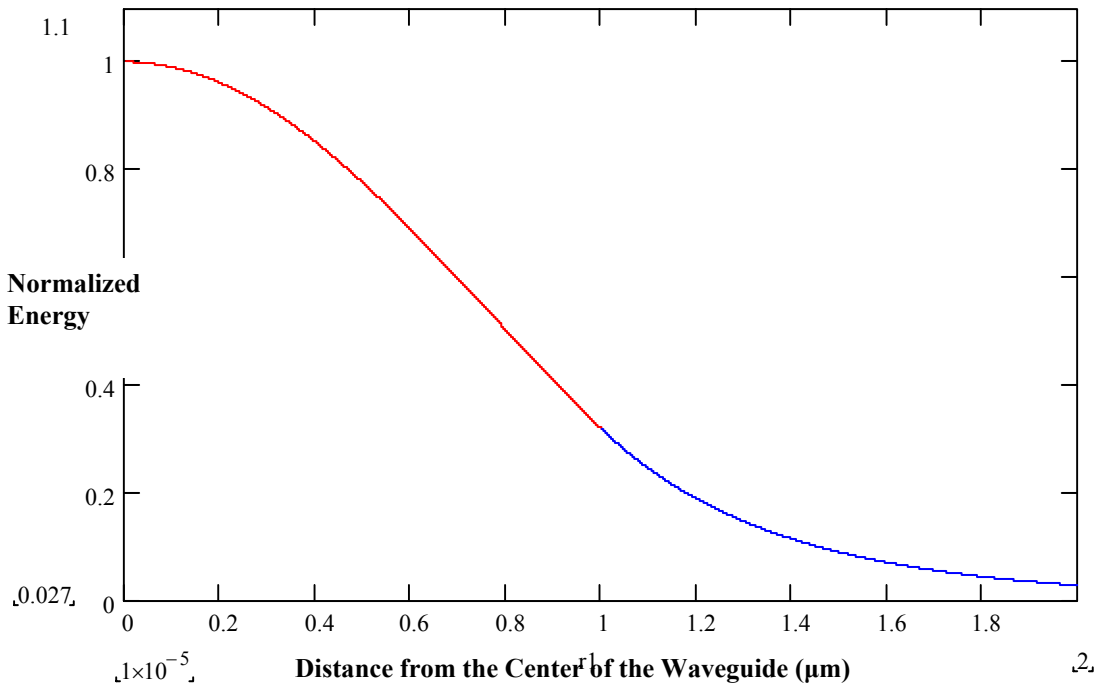

Figure 24 shows a model of the mode profile for the single-mode temperature of 60.8 °C. The red portion indicates the portion of the mode in the core, while the portion in the cladding is shown in blue.

Comparatively, it can be seen that, as temperature increases, more of the mode extends into the cladding. This is quantified by the program, which calculates that only 62.6896 percent of the energy is contained in the core at this higher temperature.

However, as the sample temperature continues to increase and nears an index of refraction match of the waveguide core and cladding, an interesting phenomenon is observed. The mode profile at a temperature of 66.5 °C is shown in Figure 25.

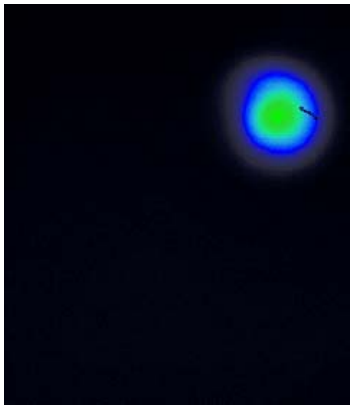

Figure 25 shows the mode profile for the single-mode temperature of 66.5 °C.

This data can also be fit to the computer generated model to determine the effective beam diameter at this temperature, as shown in Figure 26.

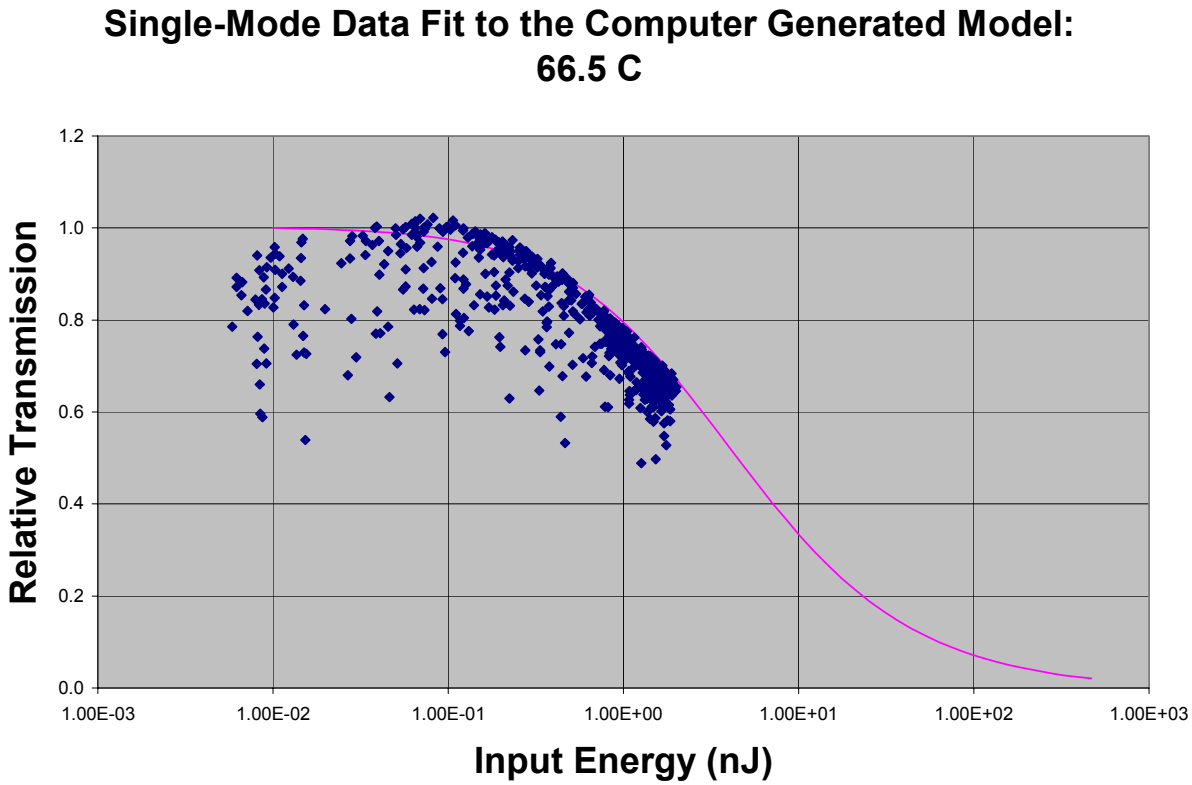

Figure 26 shows the single mode data at 66.5 C. This data is fit to a theoretical model using the computer generated model.

This yields an effective beam diameter of 2.2 μm. This shows that, as the core and the cladding near index match, this trend of optical limiting decreasing with temperature reverses itself. This is possibly the result of light being lost to the exterior of the cladding at these broad mode distributions.

The mode distribution will again be modeled using the Mathcad program.

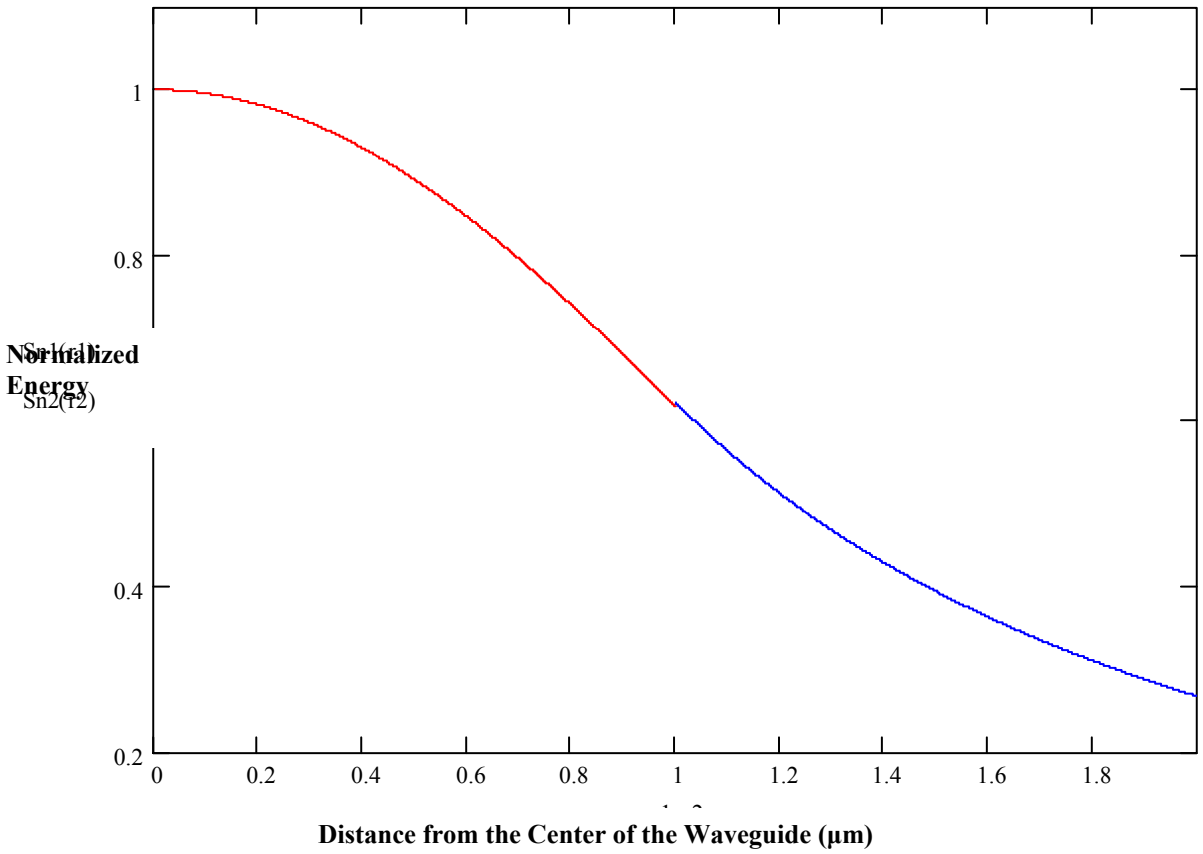

Figure 27 shows a model of the mode profile for the single-mode temperature of 66.4658 °C. The red portion indicates the portion of the mode in the core, while the portion in the cladding is shown in blue.

The program reveals that only 15.1 percent of the energy is in the core at this temperature. This is the result of the mode profile becoming broader and extending further into the cladding at

higher temperatures where the core and the cladding have a smaller difference in index of refraction.

D. Compiled Data Considering Energy in Core

It is also interesting to reinterpret the data to examine relative transmission as a function of energy only in the core. This treatment is shown below in Figure 28.

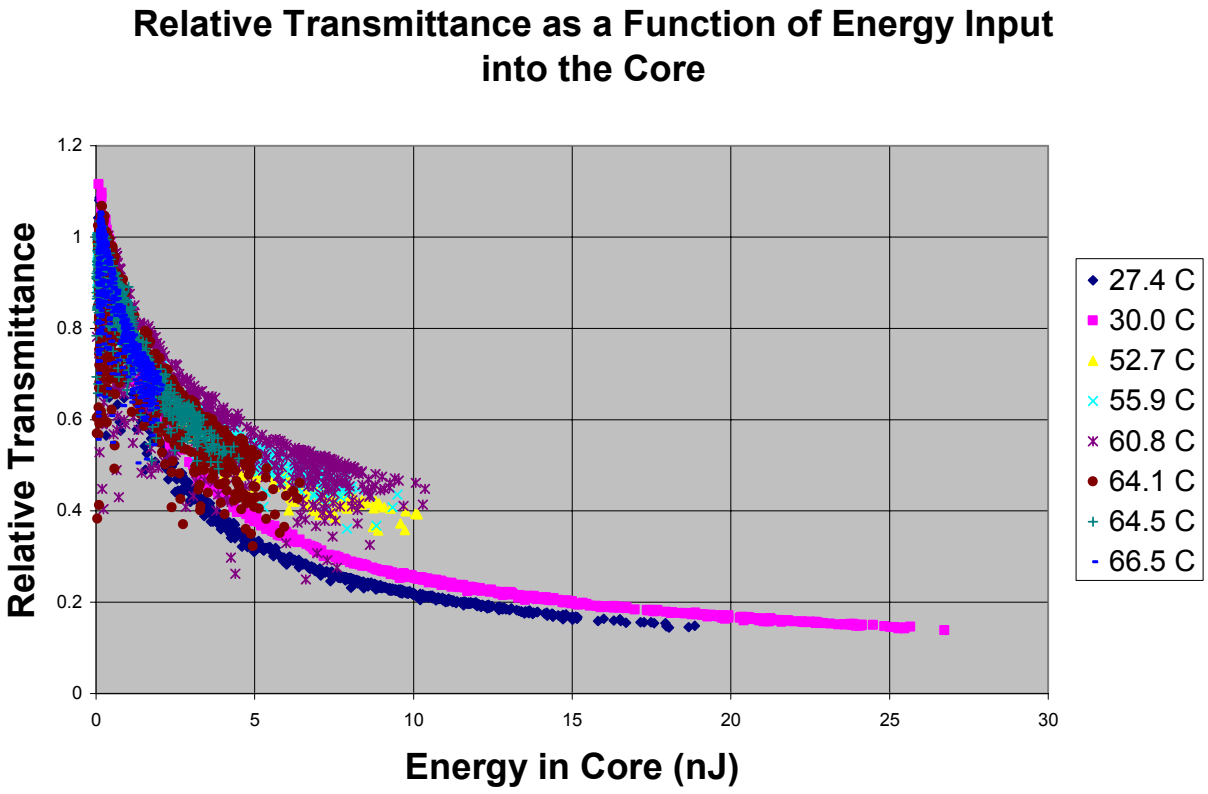

Figure 28 shows the compiled set of data in which relative transmission is graphed as a function of only the energy in the core. This data reveals that, at high single-mode temperatures that cause the index of refraction of the core and cladding to be nearly matched, the optical limiting improves. This may be the result of light being lost to the exterior of the cladding at broad mode profiles.

This reveals that in a single-mode waveguide, for a given energy in the core, approximately the same amount of limiting occurs at any single-mode temperature. However, as the temperature of

the sample increases, the difference in the index of refraction between core and cladding decreases. This leads to the mode profile within the core being spread over a wider area. Since the energy density drops slightly, a small decrease in the amount of optical limiting exhibited by the waveguide is observed.

It should also be noted that this trend reverses itself at the single mode sample temperature of 64.1 °C. It is possible that this occurs because, at this index difference, a portion of the mode structure is lost to the exterior of the cladding.

8. Conclusions

From this study, it can be concluded that multi-mode waveguides exhibit better optical limiting than single-mode waveguides. This is due to the fact that, in a multi-mode waveguide, the entire mode structure is confined to the core. Conversely, in a single-mode waveguide, a portion of the mode extends into the cladding and is not limited.

In addition, it is observed that single mode waveguides exhibit roughly the same amount optical limiting at a given input energy in the core. However, as the temperature increases and the difference in index of refraction between the core and cladding decreases, there is a decrease in the ability of waveguide to limit. This is the result of the mode profile in the core becoming broader, reducing the optical energy density within the core.

However, as the core and cladding near index match, this trend reverses itself and the single-mode waveguide exhibits improved optical limiting. This is possibly due to some of the light being lost from the mode profile to the exterior of the cladding.

9. Future Work

While the collected data was useful in drawing conclusions, there is a significant amount of scatter in the data. It is believed that this is the result of oscillations in the capillary causing fluctuations in the coupling efficiency. The test sample sits between a heater plate and open air. It is possible that convection currents caused by this temperature gradient are causing these fluctuations. It is also possible that these convection currents are causing fluctuations in the index of refraction of the air in front of the waveguide, creating a mirage effect and scattering the data. This problem may be solved if another heating plate is placed above the sample to reduce this temperature gradient and thus these currents. Once this is accomplished, the data could be retaken with less scatter at higher temperatures.

The data analysis could also be improved by rewriting the Fortran program in such a way that it does not assume that the entire mode structure is in the core, but rather accounts for the portion of the mode structure that extends into the cladding. This would give a more accurate fit of the data to a theoretical model.

When these enhancements are made, this study will serve as the ground work for a follow up study of optical limiting in coupled waveguide cores. If two waveguide cores are coupled close enough together, it will be possible to couple light from one waveguide to another via the mode's evanescent field. Optical limiting in such a system has not yet been characterized.

Bibliography

1. James S. Shirk, *Protecting the War Fighter's Vision In a Laser-Rich, Battlefield Environment,* Optics and Photonics News, April 2000.

2. Richard L. Sutherland, *Handbook of Nonlinear Optics*, p. 619. University of Rochester, New York, 1992.

3. Paul A. Tipler, *Physics Forth Edition Volume 2*. W.H. Freeman and Company. New York, 1990.

4. Robert W. Boyd, *Nonlinear Optics*, p. 16. The Institute of Optics, University of Rochester, New York, 1992.

5. Jeremiah J. Wathen, *Optical Limiting Within Capillary Waveguides*. Trident Series.

6. I.C. Khoo, *Chemical Physics*. **245**, 517-531 (1999).

7. James S. Shirk, et. al., *Mat. Res. Soc. Symp. Proc.*, Vol. 374, 1995.

8. J.W. Perry, et. al., *Optics Letters*, Vol. 19, No 9, 1994.

9. Gerd Keiser, *Optical Fiber Communications*. (McGraw-Hill, Inc., 1991).